Published in final edited form as:
Biomaterials. 2006 October ; 27(28): 4846–4855.

The effect of RGD fluorosurfactant polymer modification of ePTFE on endothelial cell adhesion, growth, and function

Coby C. Larsen[a], **Faina Kligman**[b], **Kandice Kottke-Marchant**[a,b], and **Roger E. Marchant**[a,*]

a *Department of Biomedical Engineering, Case Western Reserve University, 10900 Euclid Ave., Wickenden 319, Cleveland, OH 44106, USA*

b *Department of Clinical Pathology, Cleveland Clinic Foundation, Cleveland, OH 44195, USA*

Abstract

We have synthesized and characterized a novel peptide fluorosurfactant polymer (PFSP) modification that facilitates the adhesion and growth of endothelial cells on ePTFE vascular graft material. This PFSP consists of a poly(vinyl amine) (PVAm) backbone with integrin binding Arg-Gly-Asp (RGD) peptides and perfluorocarbon pendant branches for adsorption and stable adhesion to underlying ePTFE. Aqueous PFSP solution was used to modify the surface of fluorocarbon substrates. Following subconfluent seeding, endothelial cell (EC) adhesion and growth on PFSP was assessed by determining cell population at different time points. Spectroscopic results indicated successful synthesis of PFSP. PFSP modification of ePTFE reduced the receding water contact angle measurement from 120° to 6°, indicating successful surface modification. Quantification of cell population demonstrated reduced EC attachment efficiency but increased growth rate on RGD PFSP compared with fibronectin (FN). Actin staining revealed a well-developed cytoskeleton for ECs on RGD PFSP indicative of stable adhesion. Uptake of acetylated low-density lipoprotein and positive staining for VE-Cadherin confirm EC phenotype for adherent cells. Production of prostacyclin, a potent antiplatelet agent, was equivalent between ECs on FN and RGD PFSP surfaces. Our results indicate successful synthesis and surface modification with PFSP; this is a simple, quantitative, and effective approach to modifying ePTFE to encourage endothelial cell attachment, growth, and function.

1. Introduction

Cardiovascular disease, including coronary artery disease, is the leading cause of mortality in the United States, responsible for 494,000 deaths in 2002 [1]. Over 515,000 coronary artery bypass graft procedures are performed each year in the U.S. to replace diseased, atherosclerotic vessels [1]. Autologous vessels are the replacement conduit of choice for small-diameter bypass, yet in 30–40% of these patients satisfactory vessels are absent or inadequate [2]. Even when the autologous vessels are available, long term patency ranges from 50–90% and autologous vessel harvest incurs extra cost and patient morbidity. This underscores the need for a suitable small-diameter (<5 mm diameter) artificial vascular graft.

Currently used vascular graft materials, such as expanded polytetrafluoroethylene (ePTFE), suffer from early occlusion and thrombosis, and late intimal hyperplasia when employed in small-diameter applications [2,3]. One approach to improve the biocompatibility of small-diameter ePTFE vascular grafts is to facilitate the formation of a lumenal monolayer of autologous endothelial cells (ECs). ECs, a vital component of normal vasculature, have important antiplatelet, anticoagulant and profibrinolytic properties [4–7]. A confluent

*Corresponding author. Tel.: +1-216-368-3005; fax: +1-216-368-4969 E-mail address: roger.marchant@case.edu (R.E. Marchant)

monolayer of ECs exhibiting an antithrombotic phenotype on the graft lumen would serve to eliminate the primary mechanism of vascular graft failure.

An important consideration with ePTFE graft material is how to facilitate stable EC attachment. Without modification, ePTFE grafts show attachment of only 10 ± 7% of applied ECs, with EC retention of only 4 ± 3% [8,9]. One method for promoting EC attachment is to coat the surface with a thin protein layer (e.g., fibronectin) [10,11]. However, the adsorption and adhesion of the protein on unmodified ePTFE is limited due to interfacial characteristics; the use of biological materials is also associated with the risk of pathogen transfer, formation of thrombi, and immune reactions [10]. Another approach focuses on modification of graft surfaces with domains in naturally occurring extracellular matrix (ECM) proteins, especially the Arginine-Glycine-Aspartic Acid (RGD) sequence, for specific interactions with integrin cell-surface receptors. RGD peptides immobilized directly onto many materials have demonstrated enhanced EC attachment [12]. For inert fluoropolymers, surface modification techniques such as plasma [13] or photochemical treatment [10] have been used to introduce a diverse set of functionalities for peptide attachment [14], but these methods allow little control over peptide orientation and spacing.

An alternative route to produce RGD functionalized graft surfaces is to use a surfactant adsorption technique, allowing surface modification by a simple dip coating process. Peptides are immobilized covalently to the hydrophilic head group; a fluorocarbon tail acts as a ‘hydrophobic anchor’ to the underlying fluorocarbon surface [15]. This approach most commonly utilizes small, perfluorinated molecules; however, without crosslinking, these peptide fluorosurfactants lack the stability of higher molecular weight modifications.

Our previous work demonstrated that high molecular weight oligosaccharide-fluorocarbon surfactant polymers could successfully modify PTFE surfaces for reduction of nonspecific protein adsorption. This was accomplished by attaching hydrophilic oligosaccharides and hydrophobic perfluorodecanoyl groups to a poly(vinyl amine) (PVAm) backbone [16]. The present work extends the application of fluorocarbon surfactant polymers by inclusion of pendant cell adhesive RGD peptides. This peptide fluorosurfactant polymer (PFSP) consists of a flexible PVAm backbone with cell adhesive RGD peptides and hydrophobic perfluoroalkanoyl side chains for facilitating polymer self-assembly on fluorocarbon vascular graft surfaces. The PFSP strongly adheres to PTFE and ePTFE surfaces under aqueous conditions and provides a suitable surface for EC attachment and growth.

2. Experimental

2.1. Materials

The 9-fluorenylmethoxycarbonyl (Fmoc)-protected amino acids were obtained from AnaSpec (San Jose, CA). The solvents for peptide synthesis included N,N-dimethylformamide (DMF), dichloromethane, 20% piperidine/DMF, diisopropylethanolamine, and trifluoroacetic acid; resin (Fmoc-PAL-PEG-PS) and activator O-(7-azabenzotriazol-1-yl)-1,1,3,3-tetramethyluronium hexafluorophosphate were purchased from Perseptive Biosystems (Framingham MA). Perfluorodecanoic acid, N-hydroxysuccinimide, dicyclohexylcarbodiimide (DCC), and sodium cyanoborohydride ($NaCNBH_3$) were purchased from Aldrich (St. Louis, MO); glutaraldehyde (25% water solution) was purchased from Fluka (Switzerland); 1H, 1H, 2H, 2H-Perfluordecyl-trichlorosilane was purchased from United Chemical Technology, Inc. (Bristol, PA). DMF, dimethyl sulfoxide (DMSO) and hexadecane were purchased from Aldrich and purified by vacuum distillation before use. Water was purified through Millipore filtration system producing water with resistivity higher than 18.2 MΩ-cm. Poly(vinyl amine) (PVAm, Mn = 11,000) was prepared as reported previously [17]. Polytetrafluorethylene (PTFE, skived thin sheet) was obtained from Enflo Inc. (Bristol, CT).

Medical grade ePTFE tubing (internal diameter 0.8 μm, wall thickness 0.005 μm, internodal distance 20–30 μm) was obtained from ZEUS (Orangeburg, SC). All other reagents and solvents were used as received, unless specified otherwise.

2.2. Characterization

Molecular weight analysis of peptides was performed using a PerSeptive Biosystems matrix-assisted laser desorption/ionization time-of-flight spectrometer (MALDI-MS) using a Voyager Biospectrometry Workstation. ^{1}H-NMR spectra were obtained on a Varian Germini-200 MHz spectrometer using D_2O or DMSO-d_6 as a solvent. FTIR spectra in the range 400–4000 cm^{-1} were recorded using a Bio-Rad Digilab FTS-40 IR spectrometer. For IR analysis, the materials were ground with KBr and pressed into pellets. For each sample, 100 scans were collected with a resolution of 8 cm^{-1}. X-ray photoelectron spectra (XPS) were collected on a Physical Electronics PHI-5400 X-ray photoelectron spectrometer with monochromatic Aluminum Ka radiation source, at 250 W (from a 15kV electron emission).

Advancing and receding water contact angles were measured with a Rame-Hart contact angle goniometer (Mountain Lakes, NJ) by the sessile drop method [17]. Each reported angle represents an average ± standard deviation of at least 6 measurements. Surface tension was measured by the Du Nouy ring method, using a Sigma 703 surface tensiometer at 25ºC. The tensiometer was calibrated with pure water before each use. The surface tension of each solution was measured 3 times at each concentration 1 h after dilution to allow time for equilibration. Reproducibility was within ± 1.0 dyn/cm.

RGD density on PFSP was estimated in a similar manner as previously described [18]. Briefly, Biosym molecular modeling software (Molecular Simulations, San Diego, CA) was used in conjunction with XPS composition data for the PFSP to calculate the peptide spacing. The software was used to model two cases for PVAm backbone spacing after assembly of the PFSP on a fluorocarbon substrate- one assuming complete interdigitation of the perfluorocarbon side chains on neighboring PVAm backbones, and one assuming the nearest proximity of neighboring PVAm backbones without any interdigitation of perfluorocarbon side chains.

2.3. Polymer synthesis

The general synthetic strategy is based on PVAm chemistry and is depicted in Figure 1. PVAm (Mn=11,000) was synthesized as described previously [17]. Briefly, N-vinyl formamide was polymerized by free radical methods in isopropanol for 4 h at 60ºC, using AIBN (2,2-azobisisobutyronitrile) as the initiator.

2.3.1. Peptide—The cell adhesive peptide (GSSSG**RGD**SPA) and its negative control analog (GSSSG**RGE**SPA) were synthesized using a PerSeptive Biosystems (model 9050) solid-phase peptide synthesizer (Applied Biosystems, Foster City, CA). Fmoc methodology, common solvents, packing resin and capped amino acids were utilized. The peptide was then deprotected and cleaved from the resin, purified by preparatory scale high performance liquid chromatography (HPLC), and characterized for composition by mass-spectroscopy (one major peak at m/z=977.3 for RGD-peptide and 990.9 for RGE-negative control peptide).

2.3.2. Peptide-aldehyde conjugate—Cleaved and purified peptide (50 mg, 0.051 mmol) was reacted with glutaraldehyde (25 mg, 0.25 mmol) using the Schiff base reaction by coupling a primary amine (peptide N-terminus) with an alkyl aldehyde in a presence of catalyst, $NaCNBH_3$ (3.24 mg, 0.051 mmol), in aqueous solution. The aldehyde-terminated peptide (Pepald, 33 mg, 0.031 mmol) was purified from excess glutaraldehyde by reverse phase-HPLC and dialysis, and lyophilized. ^{1}H-NMR spectrum in DMSO-d_6: 9.7 ppm (CHO), 7–8.5 ppm (amide backbone) and peaks in 1.2–5.2 ppm region assigned to peptide's side groups' protons.

2.3.3. Peptide attachment to polymer chain—Reactive glutaraldehyde-modified RGD-peptide (33 mg, 0.031 mmol) was attached to PVAm (2.22 mg, 0.051 mmol) as described above. The product (25 mg, 0.022 mmol peptide) was purified by extensive dialysis against water for 48 h, lyophilized and characterized by FTIR and ^{1}H-NMR. IR (KBr, cm^{-1}) 3305 (*v* (OH), 2926–2968 (*v* (CH) of CH_2 and CH), 1650 (amide-I) and 1547 (amide-II). No residual aldehyde peak (at 9.7ppm) was present in the ^{1}H-NMR spectrum.

2.3.4. N-(Perfluoroundecanoyloxy) succinimide—DCC (0.86 g, 4.2 mmol) was added to a solution of perfluoroundecanoic acid (2 g, 3.5 mmol) and N-hydroxysuccinimide (0.48 g, 4.2 mmol) in DMF (5 ml). The mixture was stirred at ice bath temperature. After 5 h, the reaction mixture was filtered to remove the dicyclohexyl urea, and the precipitate was washed with cold DMF (10 ml). The solvent in the filtrate was removed by vacuum rotary evaporation. The yellow, oily residue was washed with water and chloroform to yield a white solid. This product was vacuum dried at room temperature to give 1.64 g (70%) of N-(perfluoroundecanoyloxy) succinimide. IR (KBr, cm^{-1}): 1774 (C=O) of ester), 1705 and 1659 (C=O of imide), 1214 and 1152 (-CF_2-).

2.3.5. Fluorocarbon attachment to polymer chain—The N-(perfluoroundecanoyloxy) succinimide (9.3 mg, 0.0146 mmol in 1 ml methanol) was added to PVAm-Pep (25 mg) dissolved in 2 ml DMSO and stirred for 5 h at room temperature. The initial molar ratio of peptide to fluorocarbon was 1.5:1. The final product was purified by extensive dialysis against water and lyophilized (16 mg). IR (KBr, cm^{-1}) 3305 (*v* (OH), 2926–2968 (*v* (CH) of CH_2 and CH), 1650 (amide-I) and 1547 (amide-II), 1224 and 1154 (-CF_2-). XPS atomic composition data on polyethylene: O 18.7%, N 12.9%, F 12.4%.

2.4. Fluorocarbon self-assembled monolayer

Self assembled monolayers of perfluorosilanes (FSAM) on glass cover slips were employed as a model substrate for PFSP modification. The optically transparent FSAM substrate permitted phase contrast microscopy of adherent ECs. To fabricate FSAM surfaces, 18-mm diameter glass cover slips were cleaned by sonication in fresh chloroform for 30 min. The cover slips were then treated in a radio frequency plasma reactor (Branson/IPC PM 118, 50 W, 0.5 Torr) with argon/water vapor for 15 min on each side to create a surface with hydroxyl groups. FSAMs were formed by immersing clean substrates in freshly mixed 1% (v/v) perfluorodecyl trichlorosilane in hexadecane for 30 min on each side. FSAM surfaces were then sonicated in fresh chloroform 3 times for 10 min with a fresh chloroform rinse after each sonication. Atomic force microscopy surface roughness profiling confirmed the smoothness of the surface (R_a=0.19 nm).

2.5. Surface modification

The surfactant polymer was dissolved in water (2 mg/ml) and adsorbed on FSAM, PTFE, and ePTFE for 24 h. The samples were removed from the solution and dried. PFSP stability on PTFE, ePTFE, and FSAM was tested under water for up to 4 weeks. Upon removal, samples were rinsed 3 times with pure water and dried at room temperature for 24 h. The degree of PFSP modification and stability was determined by water contact angle measurements and XPS analysis.

2.6. Culture of human pulmonary artery endothelial cells

Human pulmonary artery endothelial cells (ECs; Cambrex, Walkersville, MD) obtained at passage 3 were grown to 80–90% confluence from a 1:3 split ratio in 25 cm^2 polystyrene tissue culture flasks (Costar, Boston, MA) coated with human fibronectin (FN, Sigma, 1 μg/cm^2) in complete growth medium (CGM) and trypsinized using trypsin/EDTA (BioWhittaker;

Walkersville, MD). Culture medium was made by supplementing basal media (MCDB 131, Sigma) with 0.015% (w/v) EC growth factor supplement (ECGS, Core Facilities Laboratory, Cell Biology Department, Cleveland Clinic Foundation, Cleveland, OH), 0.009% heparin (w/v, heparin activity, 16.3 U/mL; isolated from porcine mucosa, Sigma) and 10% (v/v) fetal bovine serum (FBS; Sigma). ECs for experiments were used at passages 6–9.

2.7. Endothelial cell studies

2.7.1. Adhesion and growth assessment—Confluent ECs were trypsinized and resuspended in serum-free Opti-Mem I (Gibco; Invitrogen) for seeding at a subconfluent density (via hemocytometer count) of 15,000 cells/cm^2. Experimental surfaces included both RGE-PFSP on ePTFE (n=2/time point) and RGD-PFSP modified FSAM (n=2/time point), ePTFE (n=6/time point), and PTFE (n=2/time point); these surfaces were sterilized at room temperature by a 5 h exposure to ethylene oxide followed by a 24 h outgassing period. FN coated glass (1 μg/cm^2) surfaces (n=7/time point) were used as the positive control and unmodified FSAM and PTFE surfaces served as negative controls; these surfaces were rendered aseptic by immersion in ethanol. ECs were permitted to attach for 2 h under controlled conditions (37°C, 5% CO_2). After 2 h, the Opti-Mem I was aspirated and replaced with CGM. Culture media was changed every 2 d. The cell population was assessed 20 h, 48 h, and 5 d after seeding by DAPI (4',6-diamidino-2-phenylindole, dihydrochloride, Molecular Probes, Eugene, OR) staining of cell nuclei and by a CellTiter proliferation assay (Promega, Madison, WI).

For the DAPI stain and count, ECs were fixed with 4% (w/v) paraformaldehyde in phosphate-buffered saline (PBS), permeabilized with 0.1% (v/v) Triton-X 100 in tris-buffered saline (TBS), and stained with DAPI (1 μM), a double-stranded DNA binding dye. For enumeration of fluorescently labeled EC nuclei, 33 epifluorescent images along 8 axes at 4 radial distances for each surface were acquired using a Nikon Diaphot 200 microscope with a 10x objective. Cells were counted automatically (ImageJ, NIH) in a 0.4 mm^2 region of interest and the average cell population was determined.

EC growth and viability were quantified using the colorimetric CellTiter Cell Proliferation Assay (Promega). The absorbance at 490 nm is directly proportional to the number of living cells. CellTiter absorbance was converted to a cell population value for data analysis using a standard linear regression for CellTiter absorbance to known cell populations.

Attachment efficiency was calculated as the ratio of attached cell density to seeded cell density. Attached cell density was calculated 20 h after initial seeding which corresponded to the end of the lag phase of cell growth; seeding density was determined by a hemocytometer count of the seeding solution. Doubling time, a reflection of cell growth rate during the logarithmic growth phase, was calculated from 20–48 h. A linear regression model was fit to natural log transformed cell population data. The time coefficient (β_1) or slope of the regression was used to obtain the doubling time parameter using this equation: $t_d = \frac{\ln(2)}{\beta_1}$.

2.7.2. Fluorescent cytoskeletal staining of endothelial cells—For examination of EC actin cytoskeleton, ECs were processed like DAPI stained surfaces except the DAPI incubation was replaced by incubation with a 1:20 solution of Alexa Fluor 488 phalloidin (Molecular Probes) in TBS for 20 min. Fluorescently labeled cells were visualized using epifluorescent illumination at 488 nm on a Nikon Diaphot 200 with a 10x objective.

2.7.3. Uptake of fluorescently labeled acetylated low density lipoprotein—To establish EC identity and function, adherent cells were incubated with 10 μg/mL acetylated low density lipoprotein, labeled with 1,1'-dioctadecyl – 3,3,3',3'-tetramethyl-indocarbocyanine

perchlorate (DiI AcLDL; Biomedical Technologies, Stoughton, MA) in Optimem I for 4 h at 37° C. Cells were then fixed and counterstained with DAPI as described in 2.7.1. DiI AcLDL uptake was visualized with a Zeiss LSM510 inverted confocal microscope using a 40X objective and a He-Ne laser for 543 nm excitation.

2.7.4. Immunofluorescent staining for VE-Cadherin—To confirm EC phenotype, adherent cells were fixed and permeabilized as described in 2.7.1. Cells were incubated overnight at 4° C in blocking solution (10 mM HEPES, 150 mM NaCl, 1 mg/ml bovine serum albumin). Blocking solution was aspirated and cells were incubated for 1.5 h with a 1:100 dilution of primary rabbit anti-VE-Cadherin antibody (Sigma) or 5 μg/ml rabbit IgG from serum (Sigma), both in TBS with 4% FBS. Cells were rinsed with TBS and incubated for 30 min. with 5 μg/ml Alexa Fluor 488 goat anti-rabbit IgG (Invitrogen) in TBS with 4% FBS. Fluorescently labeled cells were visualized using epifluorescent illumination at 488 nm on a Nikon Diaphot 200 with a 40x objective.

2.7.5. Endothelial cell production of prostacyclin—Adherent cell hemostatic function was investigated with an enzyme immunoassay kit that measures cellular production of 6-keto prostaglandin $F_{1\alpha}$ (Cayman Chemical, Ann Arbor, MI), a stable hydrolysis product of prostacyclin. To collect cell culture medium samples for assay, HPAECs (p. 7, Cambrex) were seeded on FN (1 μg/cm^2, n=3) coated glass cover slips (18 mm diameter) and RGD PFSP coated ePTFE discs (17 mm diameter, n=3) at a density of 40,000 cells/cm^2 in serum-free Optimem. After 2 h, the seeding solution was aspirated and replaced with CGM for 22 h. Medium was then aspirated and replaced with fresh CGM. After 6 h, conditioned CGM was assayed according to the manufacture's protocol using 2 dilutions and 2 replicates per dilution for each surface. Data were normalized by cell population (assessed using DAPI nuclear stain and count-see 2.7.1) on each surface and time.

2.8. Soluble RGD inhibition studies

To determine the RGD-dependence of EC interaction with the PFSP, ECs were incubated with either soluble GRGDSP or GRGESP (1 mM, Bachem, Torrance, CA) in basal media supplemented with 0.015% ECGS, 0.009% heparin, and 2 mg/ml bovine serum albumin (BSA, Sigma) for 45 min at 37°C. Peptide-incubated ECs (GRGDSP and GRGESP) were then seeded at an estimated density of 20,000 cells/cm^2 onto RGD PFSP (n=4) and FN (n=4) surfaces. After seeding for 1.5 h under controlled conditions (37°C, 5% CO_2), the EC seeding solution was aspirated and CellTiter assay was employed to determine relative cell viability.

2.9. Statistical analysis

Statistical analysis of results was performed in Microsoft Excel 2003 or Minitab 14. Two-sample t-tests assuming unequal variances were performed to compare differences in cell population at different time points or between different surfaces. A difference was considered to be significant if the two-sample t-test returned a *p*-value less than 0.05.

3. Results

3.1. Peptide fluorosurfactant polymer (PFSP) synthesis and characterization

The peptide's terminal amino group was converted to aldehyde functionality using the Schiff base reaction with excess glutaraldehyde. The aldehyde peak on ^{1}H-NMR spectra of modified peptide is distinguishable, since its chemical shift falls in the unique region of ~9.7 ppm and does not overlap with amide or peptide side group protons. The successful attachment of functionalized peptide to the PVAm backbone was confirmed by disappearance of the aldehyde peak on ^{1}H-NMR spectra of the resulting conjugate.

Perfluorocarbon pendant groups were attached to the polymer chain on the second step of the reaction using an activated form of perfluoroundecanoic acid (N-(perfluoroundecanoyloxy) succinimide) to prevent a side reaction with the unprotected aspartic acid (or glutamic acid in RGE peptide). FTIR spectroscopy confirmed fluorocarbon attachment to the polymer's backbone (Fig. 2). The IR spectra of the final surfactant polymer and PVAm-peptide conjugate were normalized to the glutaraldehyde and PVAm methylene stretch at 2942 cm^{-1}, which were taken to be constant for both products. Successful reaction of the activated perfluoroundecanoic acid with the PVAm-peptide conjugate is evidenced by bands at 1224 cm^{-1} and 1154 cm^{-1} (-CF_2-) which can be seen on the IR spectra of the final product but not on the corresponding precursor (Fig. 2). The increased relative absorbance for amide I (1650 cm^{-1}) and amide II (1547 cm^{-1}) peaks also confirm the fluorocarbon's attachment to the polymer chain.

XPS was used to estimate the peptide ligand/fluorocarbon chain ratio in the PFSP on polyethylene. Fluorine is unique to the perfluorocarbon; oxygen is unique to the peptide. By comparing these two elements, the molar ratio of the perfluorocarbon branches to peptide ligands on the polymer chain was calculated. The molar content of peptide, fluorocarbon, and unreacted amino groups on the PVAm backbone are designated as x, y, and z, respectively (Fig. 1). When we let X=%O/18 (18 oxygen atoms from peptide- the one oxygen atom from the amide linkage of perfluorocarbon to the polymer chain was neglected) and Y=%F/21 (21 fluorine atoms from fluorocarbon ligand), we get x/y=X/Y=1.7; this value is close to the initial ratio of peptide to fluorocarbon (1.5:1). The estimated RGD peptide density was 0.11 – 0.19 $nmol/cm^2$, based upon a calculation of approximately 2 peptides/nm along the PVAm backbone of the PFSP and a distance between adjacent polymer backbone chains between 1.7 and 3.1 nm depending on whether the fluorocarbon side chains were fully interdigitated or not interdigitated.

Surface tension measurements were conducted with aqueous solutions of pure RGD-peptide, RGD-peptide with glutaraldehyde spacer (Pep-ald), and PFSP (Fig. 3). Pure RGD-peptide exhibits some surface activity, slightly reducing water surface tension. Adding a glutaraldehyde spacer increases the surface activity of the peptide. The surface tension curves of the PFSP and Pep-ald are identical in the low concentration region, indicating that the decrease in surface tension in this region results primarily from the peptide-glutaraldehyde ligands. However, as the surface tension approached the value of 61–63 dynes/cm, the surfactant polymer demonstrated an increased slope. This indicates that the presence of the PVAm backbone and perfluorocarbon branches dramatically increased the surface activity at the air-water interface. The transition points may correspond to changes in polymer conformation at the interface.

3.2. Surface adsorption of peptide fluorosurfactant polymer (PFSP)

The PFSP was shown to be surface active on FSAM, PTFE, and ePTFE. The PFSP was adsorbed onto each of these substrates from an aqueous solution (2 mg/ml) for 24 h. The results depicted in Table 1 illustrate a dramatic reduction in advancing and receding water contact angles for PFSP modified substrates.

The stability of PFSP on various substrates was examined under static aqueous conditions. After 4 weeks of desorption in water, the advancing and receding water contact angles remain relatively low (Fig. 4) and XPS analysis of RGD PFSP coated PTFE surfaces remained constant (Fig. 4). This indicates that adsorption is essentially irreversible and desorption does not occur to any significant extent under aqueous conditions.

3.3. Endothelial cell studies

ECs demonstrated attachment and growth on RGD PFSP surfaces. Figure 5 demonstrates a significant increase in EC population on both FN ($p = 0.027$) and RGD PFSP ($p < 0.001$)

surfaces with time of culture. The average attachment efficiency on RGD PFSP, reflected by the difference in initial EC population, was 76% of that on FN ($p<0.02$). EC growth was more rapid on RGD PFSP compared to FN; this is reflected by a shorter EC doubling time on RGD PFSP surfaces compared with FN (40 h vs. 90 h, $p<0.001$). At 120 h or 5 days, the EC population on the RGD PFSP surfaces was 1.7 times greater than EC population on FN surfaces ($p = 0.028$). The EC population on the negative control RGE PFSP was substantially less than the EC population on FN and RGD PFSP surfaces at all time points. At 120 h, the average EC population on RGE PFSP surfaces was 1,600 cells/cm^2, an order of magnitude less than the average EC population on RGD PFSP surfaces (24,650 cells/cm^2). EC adhesion and population on unmodified FSAM and PTFE surfaces were negligible ranging from 1,800–2,600 cells/cm^2.

Figure 6a and 6d depict near confluent surface coverage by ECs on both RGD PFSP (Fig. 6a) and FN (Fig. 6d) surfaces after 120 h of culture. Cytoskeletal staining revealed well-developed, longitudinally organized actin stress fibers. ECs on RGD PFSP and FN exhibited cobblestone-like morphology typical of *in vitro* ECs. The shape and size of ECs on RGD PFSP and FN surfaces were qualitatively similar. Figure 6b and 6e illustrate comparable DiI AcLDL accumulation within the cytoplasm of adherent cells after 120 h of culture on both RGD PFSP (Fig. 6b) and FN (Fig. 6e) surfaces. Positive DiI AcLDL staining confirms EC phenotype and function on RGD PFSP [19]. Figure 6c and 6f show specific staining (arrows) for VE-Cadherin on ECs adherent to RGD PFSP (Fig. 6c) and FN (Fig. 6f). Positive VE-Cadherin staining confirms EC phenotype and confluence for RGD PFSP surfaces [20].

The results from an enzyme immunoassay for 6-keto prostaglandin $F_{1\alpha}$ production by ECs on RGD PFSP and FN are depicted in Figure 7. The average production rate of 6-keto prostaglandin $F_{1\alpha}$ for ECs on RGD PFSP (2.91x10-4 pg/cell/h) was equivalent to the rate for ECs on FN ($3.17x10^{-4}$ pg/cell/h). The R^2 value for the standard regression used to calculate concentrations was 0.884. All concentration values fell within the linear response range of the assay.

3.4. Soluble RGD inhibition studies

Figure 8 demonstrates the effect of soluble GRGDSP and GRGESP on EC attachment to RGD PFSP and FN surfaces. The RGD PFSP surfaces supported cell attachment in an RGD-dependent manner; soluble GRGDSP, but not GRGESP, inhibited EC adhesion and spreading. Preincubation of ECs with 1 mM GRGDSP prior to attachment to RGD PFSP surfaces resulted in only 34% of the CellTiter assay absorbance compared to ECs preincubated with 1 mM GRGESP ($p = 0.0002$ for difference). In contrast, pre-incubation with soluble 1 mM GRGDSP had no effect on EC attachment to FN surfaces; the CellTiter absorbance was 92% of that obtained with 1 mM GRGESP ($p = 0.2$ for difference).

4. Discussion

Fluorosurfactants exhibit unique properties that differ from hydrocarbon surfactants and display an unusually sensitive structure-activity relationship [21–24]. It has been shown that fluorosurfactants are very effective at reducing surface tension and often require an order of magnitude less product to improve wetting compared to their hydrocarbon counterparts [25]. Accordingly, we designed PFSP with relatively low perfluorocarbon pendant group content to modify the surface of fluorinated vascular graft material to promote EC attachment and growth.

The first step in attaching the RGD-peptide to the PVAm polymer backbone involved transforming the peptide into a reactive peptide-aldehyde form by reaction with glutaraldehyde. In the reaction, the molar ratio of peptide to glutaraldehyde was 1:5. An excess amount of glutaraldehyde was employed to prevent the conjugation of 2 molecules of peptide to

glutaraldehyde. To prepare peptide with terminal aldehyde functionality, the peptide was added into glutaraldehyde solution; the opposite order of addition is more likely to form a conjugate with 2 blocked aldehyde groups. The imine bonds formed during coupling were reduced to more stable amine bonds by $NaCNBH_3$. One important advantage of functionalizing the peptide's N-terminus with aldehyde is the exceptional selectivity of the reaction of an aldehyde with an amine. This allows formation of stable bonds with amino groups on the PVAm backbone without the need for an activating agent or interference with other functional groups since aldehydes do not occur naturally in amino acids. This strategy utilizes unprotected peptide; the reaction proceeds under mild conditions in aqueous solution and results in good yields.

Amide I absorbance on the final PFSP was 1662 cm^{-1}. This was only slightly shifted relative to the corresponding precursor (1658 cm^{-1}). The slight shift in the amide I peak for the PFSP stands in contrast to a more dramatic reported amide I absorbance shift for dextran-fluorocarbon surfactant polymers [15]. The reduced shift upon fluorocarbon attachment for our polymer systems results from the relatively smaller percentage of amide groups derived from perfluorocarbon attachment compared to peptide backbone.

Low surface tension enables an aqueous surfactant solution to wet and adsorb on PTFE and ePTFE [24]. The driving force for surfactant adsorption is entropic, with association between the hydrophobic perfluorocarbon pendant branches and fluorocarbon surface. Reorganization of the surface coating is expected to occur upon hydration, causing hydrophilic peptide ligands to migrate toward the water-substrate interface; the contact angle hysteresis reflects this phenomenon (Table 1). The aqueous stability of a fluorosurfactant polymer coating may be attributed to the thermodynamic compatibility of adsorbed perfluorocarbon pendant groups and entropic changes in water that reduce its penetration into the surfactant monolayer [26].

EC attachment to RGD PFSP and FN surfaces was specific, resulting from surface composition and not adsorbed media protein interaction. This was ensured by using serum-free attachment media. EC attachment efficiency on RGD PFSP was 40%; this was slightly less than the 52% EC attachment efficiency on FN surfaces. This difference may be due to ligand-integrin affinity differences for FN and RGD. Cell attachment activity is a function of attachment ligand density and affinity to cell surface receptors; attachment activity has been shown to be enhanced by higher affinity ligands [12]. FN exhibits at least two orders of magnitude higher affinity for $\alpha_5\beta_1$ integrin compared to a short, RGD-containing peptides [27]. This would give the FN surface a comparative advantage in attachment efficiency over an RGD ligand presenting surface. Another possible explanation of the higher attachment efficiency relates to the well-characterized multi-valency of EC adhesion to FN. FN is a large, complex molecule with multiple regions that interact specifically with different EC surface receptors. Thus, a full FN molecule may induce signaling events more conducive to initial cell attachment than those triggered by a surface containing only the RGD peptide.

Doubling time (t_d) is a reflection of EC growth on a surface; shorter t_d values translate into faster growth rates. Doubling time for ECs on RGD PFSP and FN surfaces were 40 h and 90 h, respectively. One explanation for the apparent proliferation rate difference relates to RGD density. As a general rule, higher RGD density is related to cell spreading, survival, focal contact formation, and to some extent, proliferation [12]. Multiple studies have demonstrated higher proliferation rates on surfaces with higher RGD peptide density [18,28,29]. Compositional data along with molecular modeling was employed to give an estimated RGD density of 0.11–0.19 nmol/cm^2 for our RGD PFSP. This is at least two orders of magnitude greater than the estimated monolayer density of FN (0.0003–0.001 nmol/cm^2) [30–32]. A molecular modeling approach to estimating peptide density has its limitations. The model assumes parallel ordering of PFSP chains and complete coverage of the substrate; additionally,

calculations do not take into account the increased surface area ePTFE has over a flat, non-textured surface with similar geometry. Despite its limitations, however, the modeling approach we have taken gives an accurate order of magnitude estimate that highlights a plausible explanation of doubling time differences for ECs on RGD PFSP versus FN surfaces. On a mechanistic level, an increase in the number of integrin-ligand bonds could be reasonably expected to increase intracellular signal transduction assembly. This assembly is actively involved in many aspects of cell behavior including proliferation and survival/apoptosis [33]. Thus, increasing the number of engaged integrins on a cell's surface by utilizing a high RGD density surface modification would be expected to enhance EC growth. The relatively fast growth rate of ECs on RGD PFSP has positive implications for vascular graft applications. Loss of seeded ECs from the surface of RGD PFSP modified ePTFE could be ameliorated by proliferation of adjacent cells. Additionally, rapid proliferation of ECs would shorten the time necessary to establish a confluent monolayer on pre-seeded graft constructs.

Endothelial cell morphology, phenotype, and function were interrogated on RGD PFSP. Well-formed and longitudinally organized actin stress fibers (Fig. 6a) infer stable attachment to RGD PFSP through focal adhesions; this predisposes adherent ECs to stable anchorage under shear stress [34,35]. Uptake of acetylated low-density lipoprotein (Fig. 6b) and positive staining for VE-Cadherin (Fig. 6c) demonstrate EC phenotype for adherent cells on RGD PFSP [36,37]. Acetylated low density lipoprotein is actively and constitutively taken up by macrophages and vascular ECs via the "scavenger cell pathway" of LDL metabolism [37]. VE-Cadherin (CD144, Cadherin 5) is an EC-specific adhesive protein connected both to the actin cytoskeleton and to the intermediate filaments [20]. It is involved in cell-cell adhesion, therefore its expression is dependent on confluence [36,38,39]. ECs retained hemostatic function on RGD PFSP. Prostacyclin (PGI_2) is a vasodilator and potent inhibitor of platelet aggregation [40]; its production is an important measure of EC hemostatic function. Due to prostacyclin's instability, the quantification of 6-keto prostaglandin $F_{1\alpha}$, a hydrolysis product, is accepted by many researchers as a surrogate measure of production [41]. Production of 6-keto prostaglandin $F_{1\alpha}$ on RGD PFSP surfaces ($2.91x10^{-4}$ pg/cell/h) was comparable to production from HPAECs on FN (Fig. 7). It was slightly less than half the rate from one report of human umbilical vein ECs (HUVECs) cultured on tissue culture polystyrene (TCPS, $6.35x10^{-4}$ pg/cell/h) but almost 3 times the rate of canine ECs on TCPS ($1.03x10^{-4}$ pg/cell/h) [42] and an order of magnitude higher than HUVEC production rate on TCPS from a different report ($7.92x10^{-6}$ pg/cell/h) [43]. Larger standard deviation from the mean 6-keto prostaglandin $F_{1\alpha}$ production rate for the RGD PFSP surfaces was likely due to a higher coefficient of variation in total cell number (25% versus 3% for FN surfaces). The varying degrees of confluence that resulted from this variation likely influenced individual EC prostacyclin production rates.

Substituting glutamic acid (E) for aspartic acid (D) in ECM mimetic peptides reduces (up to 2000 fold) their affinity for EC integrins; this translates to significant attenuation in EC adhesion to these substituted peptides [27,44]. This proved to be the case for our PFSP system with RGE PFSP failing to support EC adhesion and growth despite comparable hydrophilicity between the PFSP modified surfaces. This finding indicates that the immobilized RGD on the PFSP affects biologically specific EC attachment. The RGD dependence of EC attachment to the RGD PFSP was further established by the soluble peptide inhibition studies wherein soluble RGD inhibited EC attachment to RGD PFSP to a much greater degree than did soluble RGE. PFSP modification of ePTFE vascular graft material for endothelialization presents several advantages over clinically applied ePTFE graft modification schemes. One such modification to reach patient application involves the use of chemical alteration to the graft lumen in the form of fibrin glue to which autologous ECs can attach [45,46]. The fibrin glue coating process has been shown to suffer from thickness heterogeneity with significant fibrin deposits in 15% of grafts; these deposits, in some cases, are up to 0.8 mm thick [47]. Our PFSP modification is a monolayer coating that does not reduce cross-sectional area. Use of protein precoating to

facilitate EC adherence to graft material has been described (see ref. [48] for a comprehensive review) but has several drawbacks. Proteins isolated and purified from organisms may elicit undesirable immune responses and increase infection risks [12]. Additionally, only a fraction of the coated proteins would have proper orientation for cell adhesion due to stochastic orientation and denaturing interaction with hydrophobic graft surfaces [12]. Our PFSP modification employs small RGD peptides with controlled orientation. Small RGD peptides also exhibit higher stability in sterilization conditions, are more stable to heat treatment and pH variation, demonstrate robust storage, are easier to characterize and more cost effective [12]. Their small size permits a higher RGD density than can be achieved with monolayers of ECM proteins; this appears to compensate for the 1000 fold lower affinity than native ECM proteins [49].

5. Conclusions

A biomimetic fluorosurfactant polymer was synthesized by incorporating cell adhesive RGD peptides and fluorocarbon pendant groups on a poly(vinyl) amine backbone. The peptide fluorosurfactant polymer was shown to be surface active and to exhibit strong and stable adsorption to fluorocarbon surfaces from aqueous solution. Endothelial cells showed RGD-specific adhesion to the RGD PFSP with growth rates exceeding those of ECs on a native extracellular matrix protein. ECs adherent to RGD PFSP retained hemostatic function demonstrated by prostacyclin production. All of these data taken together indicate that PFSPs are a simple, quantitative, and effective approach to modifying ePTFE to encourage endothelial cell attachment, growth, and function. Stable endothelial cell attachment and function on PFSP modification provides tremendous promise for overcoming the early occlusion and thrombosis that have limited the use of synthetic small-diameter ePTFE vascular grafts.

Acknowledgements

The authors gratefully acknowledge the financial support provided by NIH grant 5R01EB002067 and the facilities provided by the Center for Cardiovascular Biomaterials. Graduate training support was provided for C.L. from NIH grants 5T32GM007250-30 and 5T32GM007535-28. Eric H. Anderson is acknowledged for his work in calculating PFSP peptide density.

References

1. Heart Disease and Stroke Statistics. [cited 2005 August 9]. 2005 Update. 2004 Available from: http://www.americanheart.org/presenter.jhtml?identifier=1928
2. Sayers RD, Raptis S, Berce M, Miller JH. Long-term results of femorotibial bypass with vein or polytetrafluoroethylene. Br J Surg 1998 Jul;85(7):934–8. [PubMed: 9692567]
3. Faries PL, Logerfo FW, Arora S, Hook S, Pulling MC, Akbari CM, et al. A comparative study of alternative conduits for lower extremity revascularization: all-autogenous conduit versus prosthetic grafts. J Vasc Surg 2000 Dec;32(6):1080–90. [PubMed: 11107079]
4. Cines DB, Pollak ES, Buck CA, Loscalzo J, Zimmerman GA, McEver RP, et al. Endothelial cells in physiology and in the pathophysiology of vascular disorders. Blood 1998 May 15;91(10):3527–61. [PubMed: 9572988]
5. Colman, RW. Hemostasis and thrombosis : basic principles and clinical practice. 4. Philadelphia: Lippincott Williams & Wilkins; 2000.
6. Jaffe EA. Physiologic functions of normal endothelial cells. Ann N Y Acad Sci 1985;454:279–91. [PubMed: 3907467]
7. Rodgers GM. Hemostatic properties of normal and perturbed vascular cells. Faseb J 1988 Feb;2(2):116–23. [PubMed: 3277885]
8. Kent KC, Oshima A, Whittemore AD. Optimal seeding conditions for human endothelial cells. Ann Vasc Surg 1992 May;6(3):258–64. [PubMed: 1610657]

9. Tseng DY, Edelman ER. Effects of amide and amine plasma-treated ePTFE vascular grafts on endothelial cell lining in an artificial circulatory system. J Biomed Mater Res 1998 Nov;42(2):188–98. [PubMed: 9773815]
10. Gumpenberger T, Heitz J, Bauerle D, Kahr H, Graz I, Romanin C, et al. Adhesion and proliferation of human endothelial cells on photochemically modified polytetrafluoroethylene. Biomaterials 2003 Dec;24(28):5139–44. [PubMed: 14568430]
11. Rademacher A, Paulitschke M, Meyer R, Hetzer R. Endothelialization of PTFE vascular grafts under flow induces significant cell changes. Int J Artif Organs 2001 Apr;24(4):235–42. [PubMed: 11394706]
12. Hersel U, Dahmen C, Kessler H. RGD modified polymers: biomaterials for stimulated cell adhesion and beyond. Biomaterials 2003 Nov;24(24):4385–415. [PubMed: 12922151]
13. Vargo TG, Gardella JAJ, Calvert JM, Chen M-S. Adhesive Electroless Metallization of Fluoropolymeric Substrates. Science 1993 Dec 10 1993;262(5140):1711–2. [PubMed: 17781789]
14. Neff JA, Tresco PA, Caldwell KD. Surface modification for controlled studies of cell-ligand interactions. Biomaterials 1999 Dec;20(23–24):2377–93. [PubMed: 10614943]
15. Goessl A, Golledge SL, Hoffman AS. Plasma lithography--thin-film patterning of polymers by RF plasma polymerization II: Study of differential binding using adsorption probes. J Biomater Sci Polym Ed 2001;12(7):739–53. [PubMed: 11587038]
16. Wang SW, Marchant RE. Fluorocarbon surfactant polymers: Effect of perfluorocarbon branch density on surface active properties. Macromolecules 2004 May;37(9):3353–9. [PubMed: 16429594]
17. Qiu YX, Zhang TH, Ruegsegger M, Marchant RE. Novel nonionic oligosaccharide surfactant polymers derived from poly(vinylamine) with pendant dextran and hexanoyl groups. Macromolecules 1998 Jan;31(1):165–71.
18. Sagnella SM, Kligman F, Anderson EH, King JE, Murugesan G, Marchant RE, et al. Human microvascular endothelial cell growth and migration on biomimetic surfactant polymers. Biomaterials 2004 Mar–Apr;25(7–8):1249–59. [PubMed: 14643599]
19. Stein O, Stein Y. Bovine aortic endothelial cells display macrophage-like properties towards acetylated 125I-labelled low density lipoprotein. Biochim Biophys Acta 1980 Dec 5;620(3):631–5. [PubMed: 7236661]
20. Yap AS, Brieher WM, Gumbiner BM. Molecular and functional analysis of cadherin-based adherens junctions. Annu Rev Cell Dev Biol 1997;13:119–46. [PubMed: 9442870]
21. Eastoe J, Paul A, Rankin A, Wat R, Penfold J, Webster JRP. Fluorinated nonionic surfactants bearing either CF3- or H-CF2- terminal groups: Adsorption at the surface of aqueous solutions. Langmuir 2001 Dec;17(25):7873–8.
22. Kissa, E. Fluorinated surfactants : synthesis, properties, applications. New York: M. Dekker; 1994.
23. Muto Y, Esumi K, Meguro K, Zana R. Aggregation Behavior of Mixed Fluorocarbon and Hydrocarbon Surfactants in Aqueous-Solutions. Journal of Colloid and Interface Science 1987 Nov; 120(1):162–71.
24. Yoda K, Tamori K, Esumi K, Meguro K. Critical Micelle Concentrations of Fluorocarbon Surfactant Mixtures in Aqueous-Solution. Journal of Colloid and Interface Science 1989 Aug;131(1):282–3.
25. Arai T, Takasugi K, Esumi K. Mixed Micellar Properties of Nonionic Saccharide and Anionic Fluorocarbon Surfactants in Aqueous Solution. J Colloid Interface Sci 1998 Jan 1;197(1):94–100. [PubMed: 9466848]
26. Brezinski, D. Laying the Foundation for New Technologies. 2003 1/1/03. [cited 2005 August 15]. Available from: http://www.pcimag.com/CDA/ArticleInformation/features/BNP__Features__Item/0,1846,89696,00.html
27. Hautanen A, Gailit J, Mann DM, Ruoslahti E. Effects of modifications of the RGD sequence and its context on recognition by the fibronectin receptor. J Biol Chem 1989 Jan 25;264(3):1437–42. [PubMed: 2521482]
28. Dee KC, Andersen TT, Bizios R. Cell function on substrates containing immobilized bioactive peptides. Mater Res Soc Symp Proc 1994;331:115–9.
29. Lin YS, Wang SS, Chung TW, Wang YH, Chiou SH, Hsu JJ, et al. Growth of endothelial cells on different concentrations of Gly-Arg-Gly-Asp photochemically grafted in polyethylene glycol modified polyurethane. Artif Organs 2001 Aug;25(8):617–21. [PubMed: 11531712]

30. Pompe T, Kobe F, Salchert K, Jorgensen B, Oswald J, Werner C. Fibronectin anchorage to polymer substrates controls the initial phase of endothelial cell adhesion. J Biomed Mater Res A 2003 Nov 1;67(2):647–57. [PubMed: 14566809]

31. Kowalczynska HM, Nowak-Wyrzykowska M, Dobkowski J, Kolos R, Kaminski J, Makowska-Cynka A, et al. Adsorption characteristics of human plasma fibronectin in relationship to cell adhesion. J Biomed Mater Res 2002 Aug;61(2):260–9. [PubMed: 12007207]

32. Bhat VD, Truskey GA, Reichert WM. Fibronectin and avidin-biotin as a heterogeneous ligand system for enhanced endothelial cell adhesion. J Biomed Mater Res 1998 Sep 5;41(3):377–85. [PubMed: 9659606]

33. Giancotti FG, Ruoslahti E. Integrin signaling. Science 1999 Aug 13;285(5430):1028–32. [PubMed: 10446041]

34. Murugesan G, Ruegsegger MA, Kligman F, Marchant RE, Kottke-Marchant K. Integrin-dependent interaction of human vascular endothelial cells on biomimetic peptide surfactant polymers. Cell Commun Adhes 2002 Mar–Apr;9(2):59–73. [PubMed: 12487408]

35. Sagnella S, Kligman F, Marchant RE, Kottke-Marchant K. Biomimetic surfactant polymers designed for shear-stable endothelialization on biomaterials. J Biomed Mater Res A 2003 Dec 1;67(3):689–701. [PubMed: 14674370]

36. Lampugnani MG, Resnati M, Raiteri M, Pigott R, Pisacane A, Houen G, et al. A novel endothelial-specific membrane protein is a marker of cell-cell contacts. J Cell Biol 1992 Sep;118(6):1511–22. [PubMed: 1522121]

37. Voyta JC, Via DP, Butterfield CE, Zetter BR. Identification and isolation of endothelial cells based on their increased uptake of acetylated-low density lipoprotein. J Cell Biol 1984 Dec;99(6):2034–40. [PubMed: 6501412]

38. Angst BD, Marcozzi C, Magee AI. The cadherin superfamily: diversity in form and function. J Cell Sci 2001 Feb;114(Pt 4):629–41. [PubMed: 11171368]

39. Lampugnani MG, Corada M, Caveda L, Breviario F, Ayalon O, Geiger B, et al. The molecular organization of endothelial cell to cell junctions: differential association of plakoglobin, beta-catenin, and alpha-catenin with vascular endothelial cadherin (VE-cadherin. J Cell Biol 1995 Apr;129(1):203–17. [PubMed: 7698986]

40. Alberts, B. Molecular biology of the cell. 4. New York: Garland Science; 2002.

41. Fitzpatrick, FA., et al. Prostaglandins. In: Vane, JR.; Bergström, S., editors. Prostacyclin. New York: Raven Press; 1979. p. 55

42. Dixit P, Hern-Anderson D, Ranieri J, Schmidt CE. Vascular graft endothelialization: comparative analysis of canine and human endothelial cell migration on natural biomaterials. J Biomed Mater Res 2001 Sep 15;56(4):545–55. [PubMed: 11400132]

43. Shirota T, He H, Yasui H, Matsuda T. Human endothelial progenitor cell-seeded hybrid graft: proliferative and antithrombogenic potentials in vitro and fabrication processing. Tissue Eng 2003 Feb;9(1):127–36. [PubMed: 12625961]

44. Cherny RC, Honan MA, Thiagarajan P. Site-directed mutagenesis of the arginine-glycine-aspartic acid in vitronectin abolishes cell adhesion. J Biol Chem 1993 May 5;268(13):9725–9. [PubMed: 7683657]

45. Laube HR, Duwe J, Rutsch W, Konertz W. Clinical experience with autologous endothelial cell-seeded polytetrafluoroethylene coronary artery bypass grafts. J Thorac Cardiovasc Surg 2000 Jul;120(1):134–41. [PubMed: 10884666]

46. Meinhart JG, Deutsch M, Fischlein T, Howanietz N, Froschl A, Zilla P. Clinical autologous in vitro endothelialization of 153 infrainguinal ePTFE grafts. Ann Thorac Surg 2001 May;71(5 Suppl):S327–31. [PubMed: 11388216]

47. Fernandez P, Deguette A, Pothuaud L, Belleannee G, Coste P, Bordenave L. Quality control assessment of ePTFE precoating procedure for in vitro endothelial cell seeding. Biomaterials 2005 Aug;26(24):5042–7. [PubMed: 15769540]

48. Salacinski HJ, Tiwari A, Hamilton G, Seifalian AM. Cellular engineering of vascular bypass grafts: role of chemical coatings for enhancing endothelial cell attachment. Med Biol Eng Comput 2001 Nov;39(6):609–18. [PubMed: 11804165]

49. Ruoslahti E. RGD and other recognition sequences for integrins. Annu Rev Cell Dev Biol 1996;12:697–715. [PubMed: 8970741]

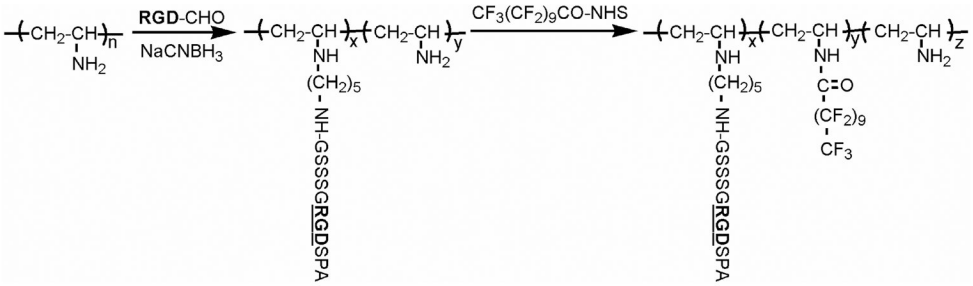

Figure 1.
Synthetic strategy for peptide fluorosurfactant polymer.

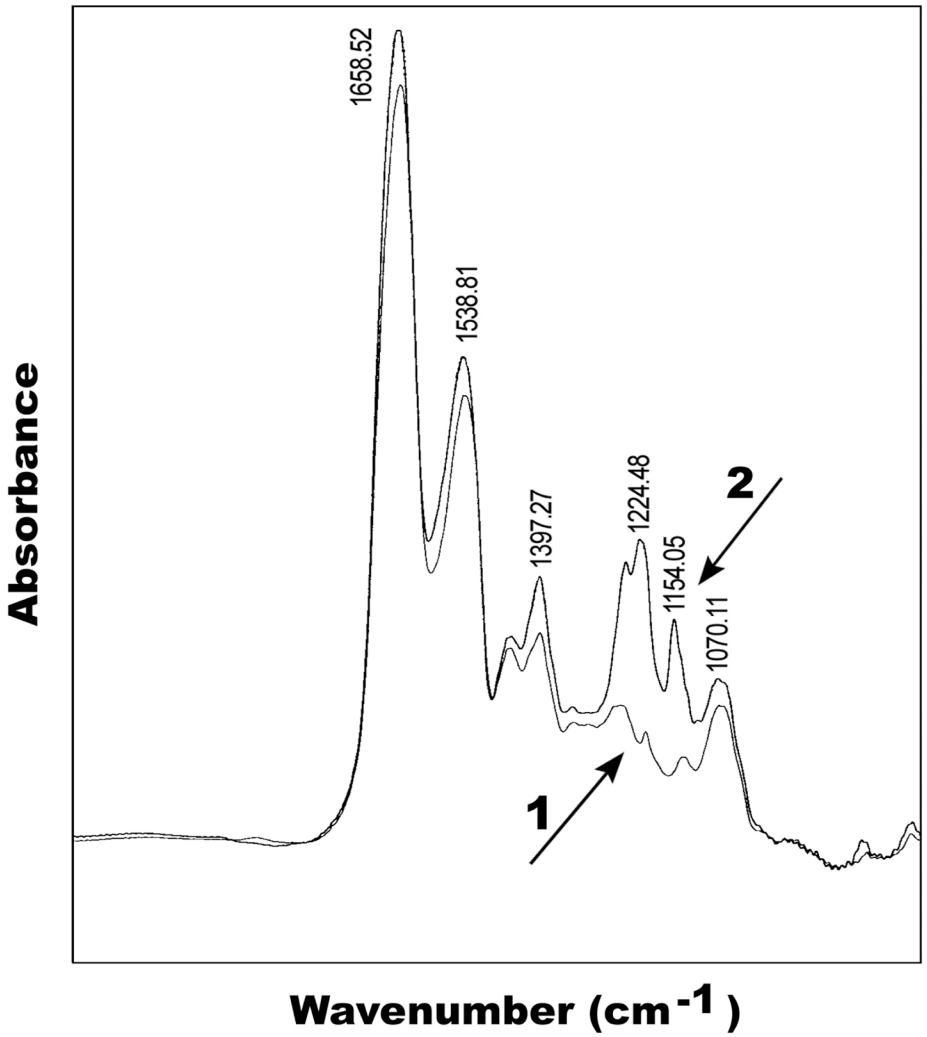

Figure 2.
IR spectra of PVAm-RGD-peptide conjugate (1) and PVAm with attached RGD peptide and perfluorocarbon (2)

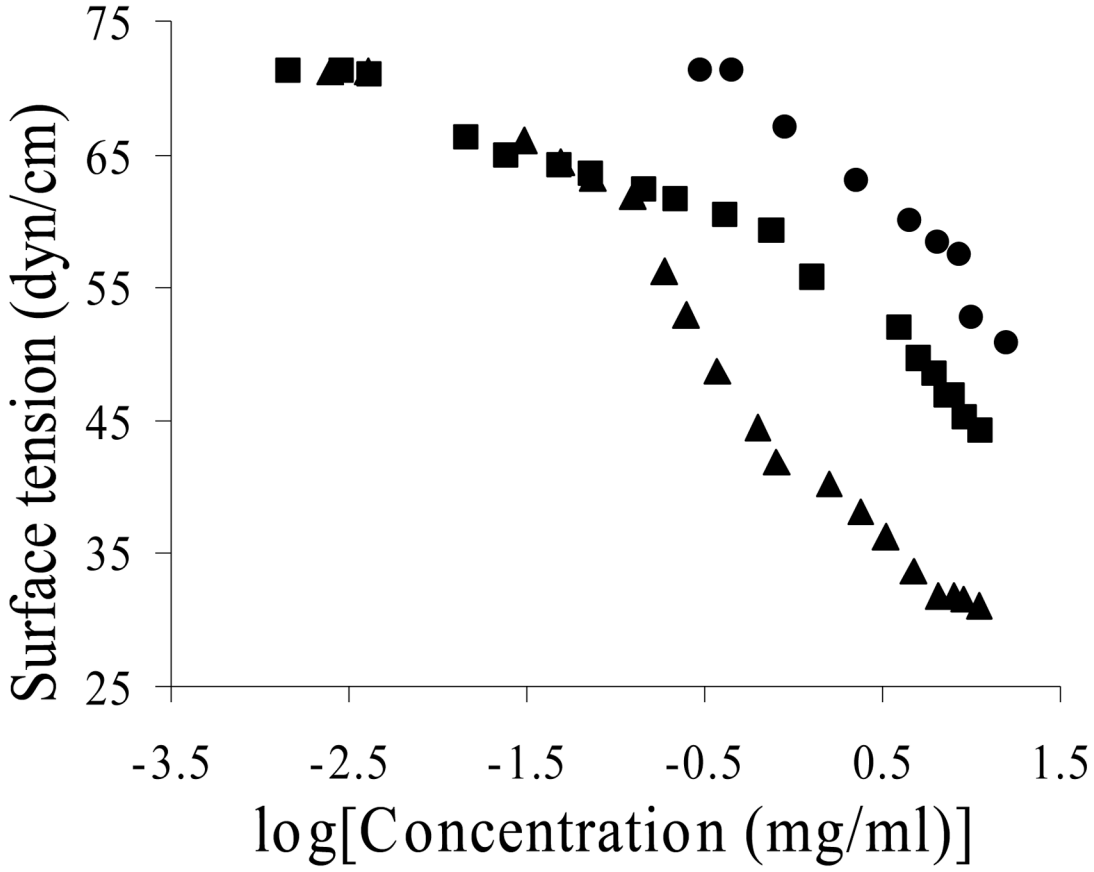

Figure 3.
Plot of surface tension versus logarithm of concentration for peptide (•), peptide-aldehyde (■), and peptide fluorosurfactant polymer (▲).

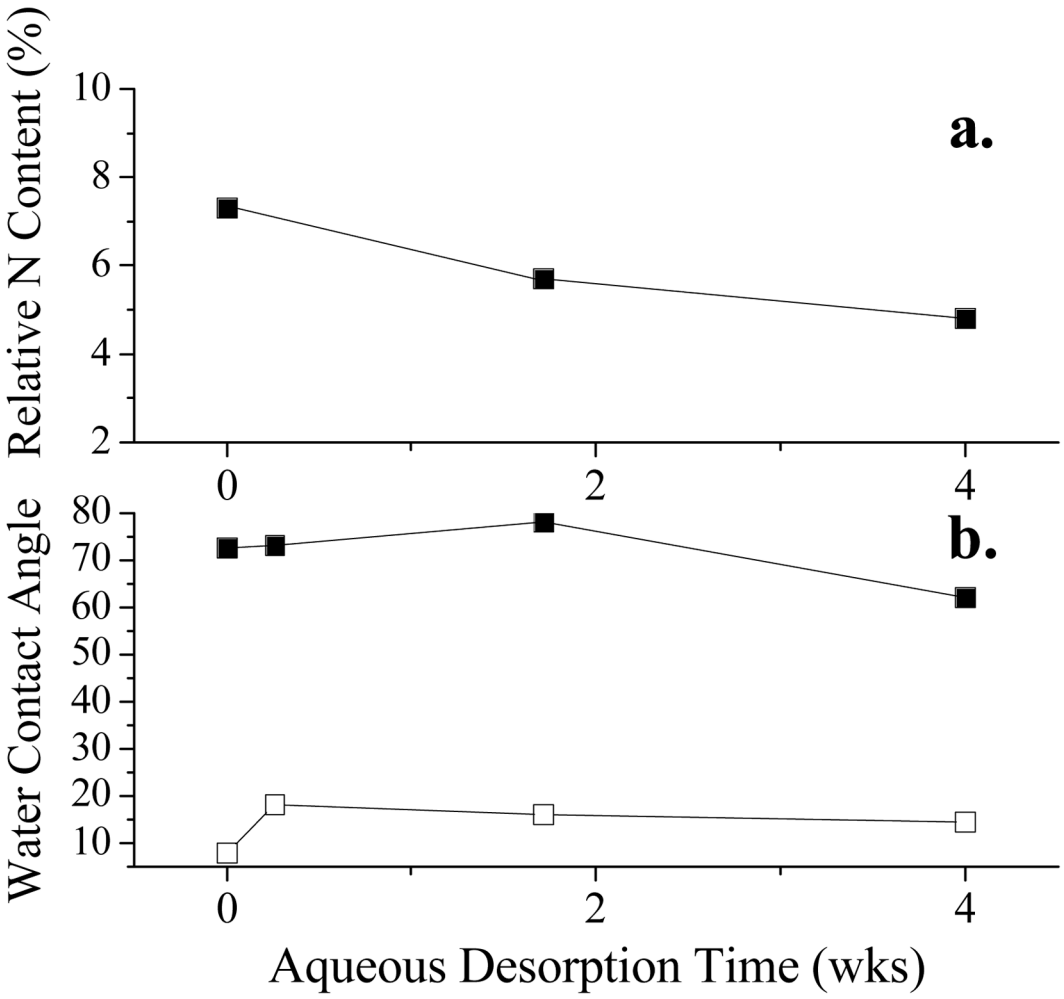

Figure 4.

Aqueous desorption stability. Change in a.) relative nitrogen content or b.) advancing (θ_a-filled symbols) and receding (θ_r-unfilled symbols) water contact angle on RGD peptide fluorosurfactant polymer on PTFE (θ_a ■, θ_r □, %N ■) after exposure to static aqueous conditions for various time lengths.

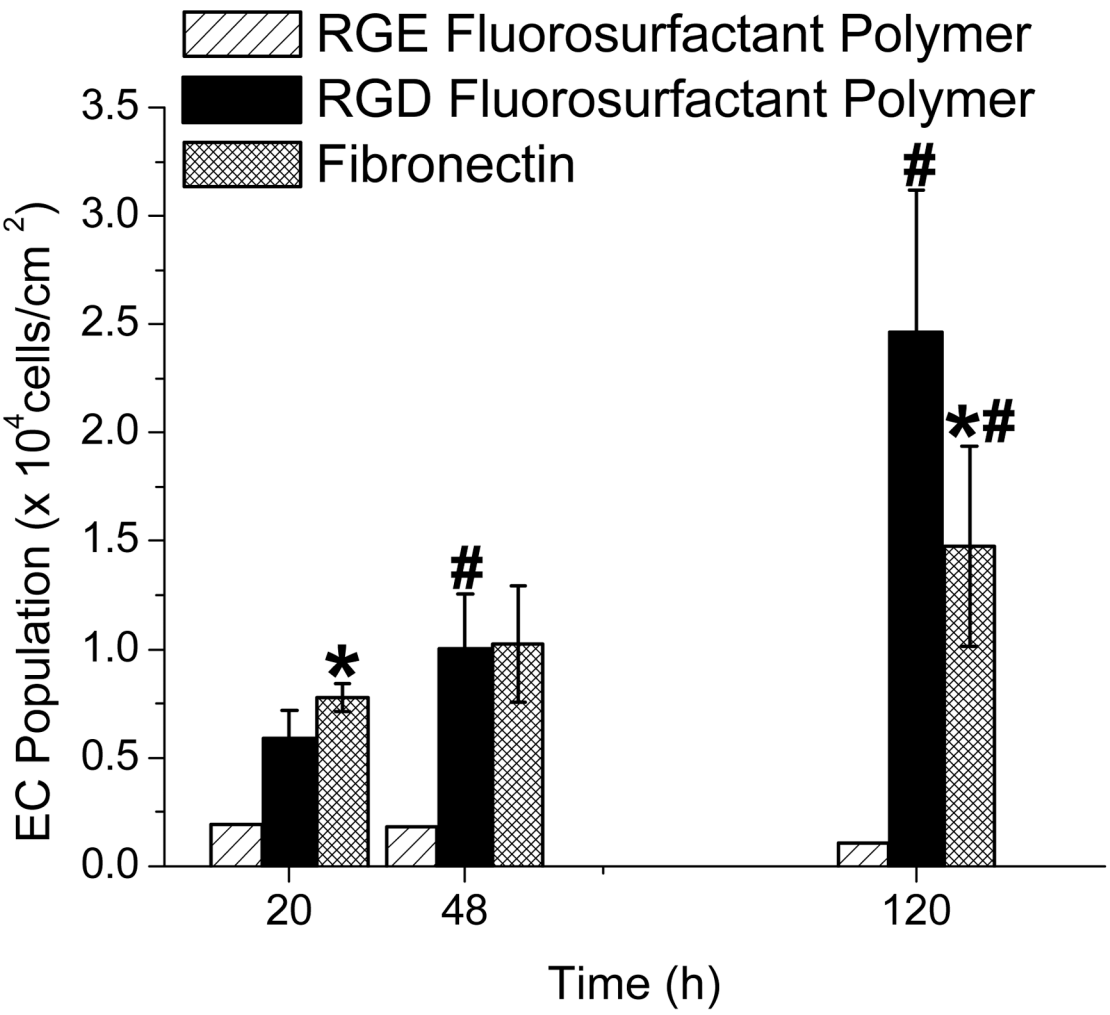

Figure 5.
EC adhesion and growth on RGE peptide fluorosurfactant polymer (PFSP), RGD PFSP, and fibronectin (FN) surfaces. * indicates difference ($p<0.05$) in EC population from RGD PFSP surface at same time point. # indicates difference ($p<0.05$) in EC population from identical surface at 20 h post-seeding. Error bars are 95% confidence intervals from 7 FN samples and 10 RGD PFSP surfaces at each time point.

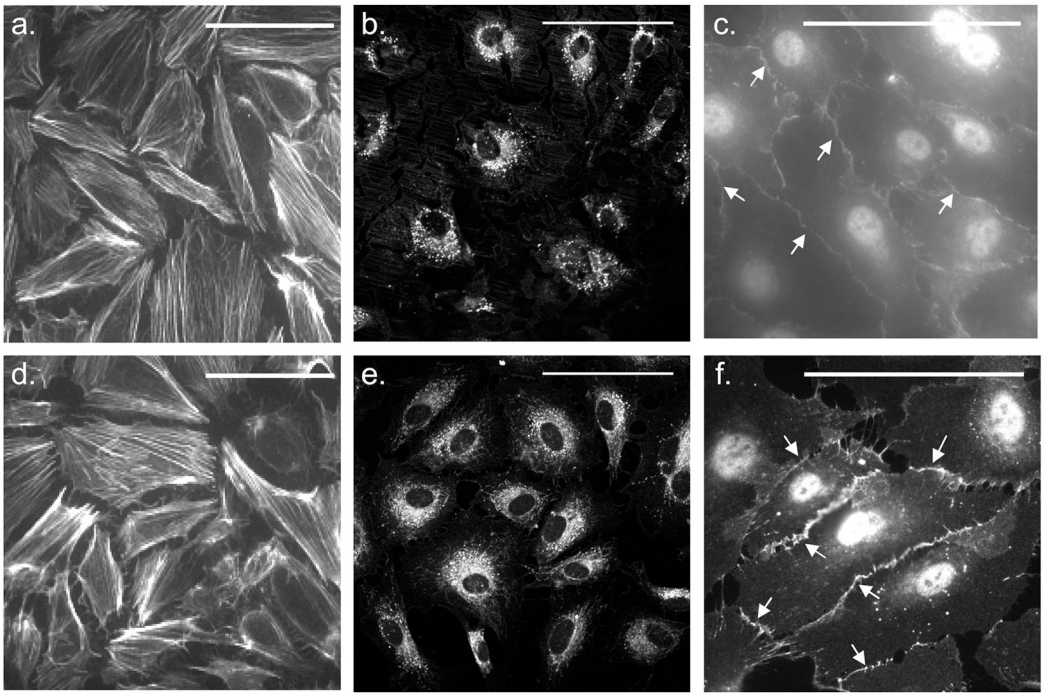

Figure 6.
EC morphology and surface coverage visualized with phalloidin (a & d), phenotype and function indicated by DiI AcLDL uptake (b & e) and VE-Cadherin staining (c & f; arrows) on RGD PFSP (a- FSAM substrate, b and c- ePTFE substrate) and FN (d–f). Scale bars are 100 μm.

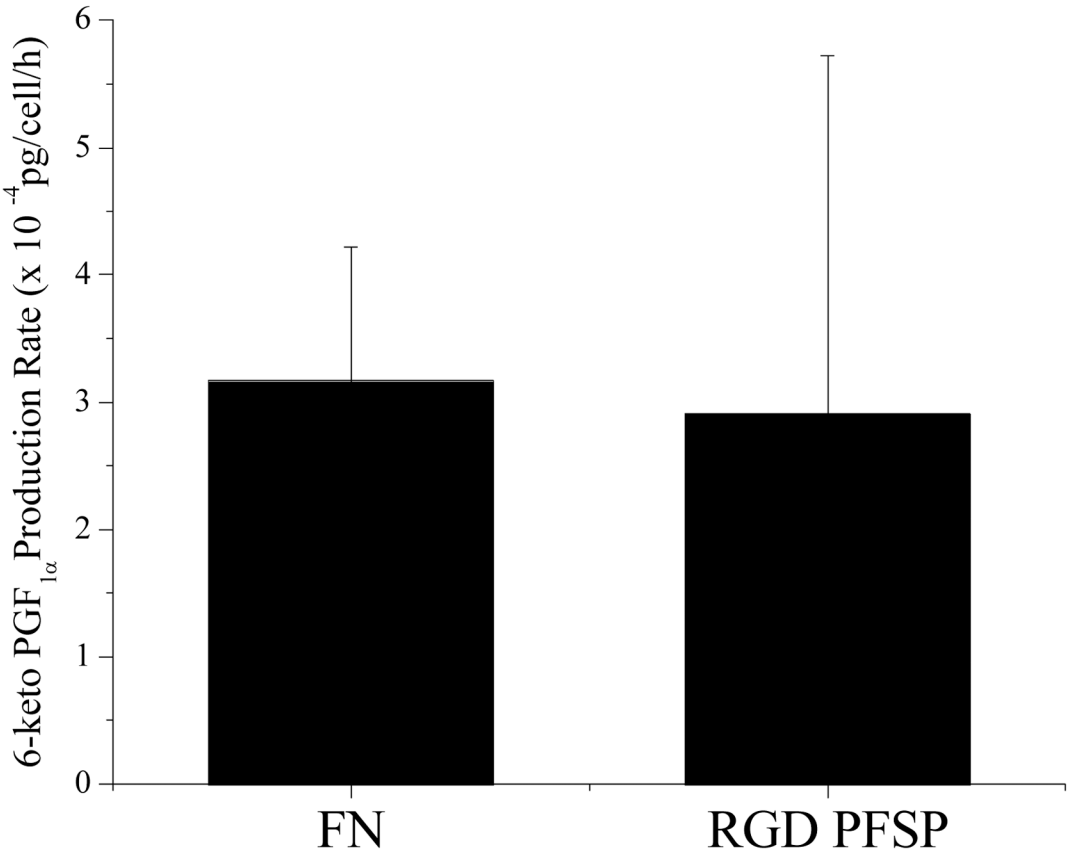

Figure 7.
Production of prostacyclin by ECs on FN and RGD PFSP measured with an enzyme immunoassay for 6-keto $PGF_{1\alpha}$, a hydrolysis product of prostacyclin. Bars represent standard deviation of 3 samples.

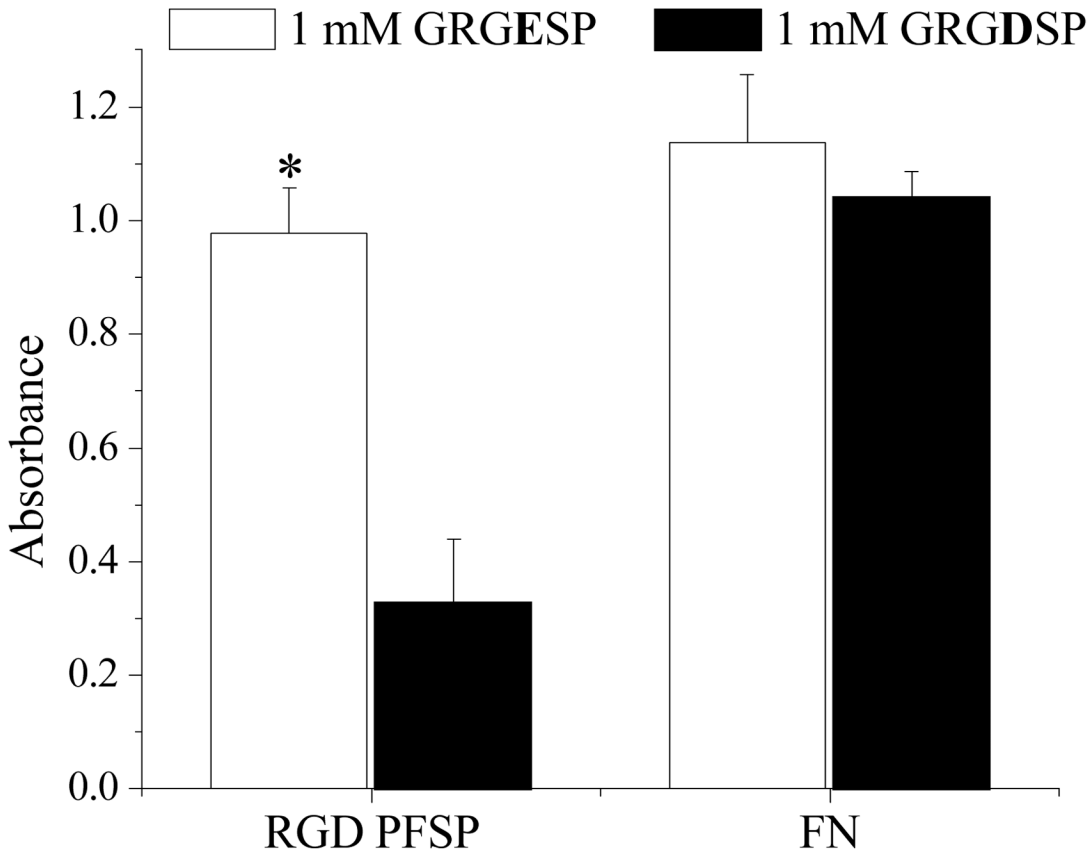

Figure 8.
Effect of soluble GRGESP or GRGDSP on endothelial cell (EC) attachment to RGD peptide fluorosurfactant polymer (PFSP) or fibronectin (FN) surfaces. ***** indicates significantly different ($p<0.001$) mean CellTiter assay absorbance compared with ECs incubated with 1 mM GRGDSP and seeded on RGD PFSP surface. Data are presented ± standard deviations from n = 4.

Table 1

Water contact angles on unmodified and peptide fluorosurfactant polymer (PFSP) modified surfaces.

Substrate	Unmodified		RGD PFSP		RGE PFSP	
	θ_a [1]	θ_r [2]	θ_a [1]	θ_r [2]	θ_a [1]	θ_r [2]
FSAM	105±2°	95±2°	35.5±3.6°	7±1°		
PTFE	110±1°	105±1°	72.5±2.5°	8±2°		
ePTFE	124±1°	120±2°	41.8±2°	6±1°	50±2°	7.1±1°

[1] Highest advancing water contact angle ± s.d. from 6 measurements.

[2] Lowest receding water contact angle ± s.d. from 6 measurements.